Self-Assembly Mediated Platform for Rapid and Facile Preparation of Peptide-Functionalized Nanoparticles with High Stability

DATASET *in* CHEMISTRY OF MATERIALS · MARCH 2012

Impact Factor: 8.35 · DOI: 10.1021/cm202860h

2 AUTHORS, INCLUDING:

Weiping Wang
Massachusetts Institute of Technology
15 PUBLICATIONS **94** CITATIONS

CHEMISTRY OF MATERIALS

Article

pubs.acs.org/cm

Self-Assembly Mediated Platform for Rapid and Facile Preparation of Peptide-Functionalized Nanoparticles with High Stability

Weiping Wang[†,‡] and Ying Chau*[,†]

[†]Department of Chemical and Biomolecular Engineering, The Hong Kong University of Science & Technology, Clear Water Bay, Kowloon, Hong Kong, China

[‡]Graduate Program of Nano Science and Technology, The Hong Kong University of Science & Technology, Clear Water Bay, Kowloon, Hong Kong, China

Supporting Information

ABSTRACT: We recently reported a two-component self-assembling system, where the core of nanoparticles (NPs) was first assembled by a simple triskelion Fmoc-conjugate (FTAEA) and then stabilized by an oligopeptide, Fmoc-FY. Here we showed that the two-component NPs were stable upon heating, incubation, and dilution. We expanded the oligopeptides suitable for stabilization and therefore allowed peptides to serve the dual role of stabilization and functionalization. Twelve molecules were systematically designed and tested to define the design criteria of oligopeptide stabilizers, which are summarized as follows: 1) carrying Fmoc headgroup to match with the aromatic groups on the NP core, 2) restricting the first amino acid to those with self-interacting side chains, and 3) the net charge of the hydrophilic oligopeptide sequence being negative. To validate these criteria, we designed two bioactive peptides, Fmoc-FC and Fmoc-FRGD, which were demonstrated to be capable of stabilizing FTAEA NPs. The bioactivity of the peptide was illustrated with Nile red-loaded Fmoc-FRGD stabilized NPs of around 70 nm in diameters. These NPs were differentially internalized by MDA-MB-435 human cancer cells compared to NPs stabilized with the scrambled sequence, Fmoc-FRDG. Our results here showed that the stepwise aromatic-driven self-assembly provided a facile and versatile approach to construct functionalized and bioactive NPs, which are expected to find applications in drug delivery and bioimaging.

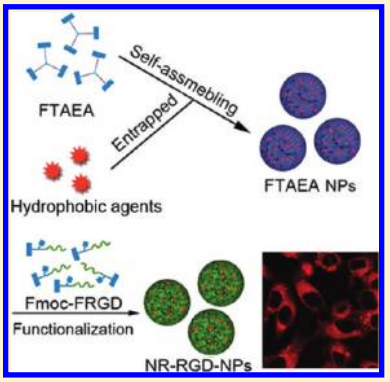

KEYWORDS: *aromatic interactions, cellular targeting, endocytosis, nanospheres, noncovalent functionalization, three-legged molecules*

INTRODUCTION

Nanoparticles (NPs) are promising candidates for biomedical applications such as bioimaging,[1−3] therapeutics,[3−5] and drug delivery.[6−9] To improve specificity against various diseased tissues, NPs are functionalized with targeting ligands to enable binding with specific cell-surface receptors, by which the cellular uptake via receptor-mediated endocytosis may also be enhanced.[7,10,11] Common targeting ligands include small organic molecules, peptides, carbohydrates, monoclonal antibodies, and aptamers.[7,12] Among these, oligopeptides are appealing because of their chemical diversity, low immunogenicity, good stability, and inexpensive production by solid phase synthesis.[13] The advance in bioinformatics with the explosion of proteomic data and chemogenomic data further facilitates the discovery of appropriate targets linked to disease biomarkers.[14] Using high-throughput screening techniques such as phage display, peptides with high affinity to specific targets can be identified.[15] Peptides are already a popular choice for NP functionalization in targeted drug delivery and imaging probes.[13,16]

However, functionalization of NPs is still a challenge for biomaterial scientists. The conventional processes involve the chemical conjugation of targeting ligands to presynthesized NPs. The ligands and the surface of the NPs must carry chemically active groups for coupling.[17,18] Besides, the coupling strategies are time-consuming and prone to side reactions, leading to high cost and limited scalability.[18] An alternative means involves the noncovalent binding of targeting ligands to the surface of NPs. However, the procedure of physical adsorption takes many hours, and the orientation of the attached ligands is difficult to control.[19−21] The competitive displacement of the adsorbed ligands by serum components or the aggregation of NPs are frequently observed, meaning that these nanoparticles lack stability.[21] Therefore, a facile and versatile approach to prepare functionalized and stable nanocarriers is of great interest and relevance to various biomedical applications. For example, a method combining layer-by-layer (LbL) assembly and click chemistry provided a promising approach to introduce covalent functionality, although it was applied on microparticles.[22,23]

Recently, we showed a facile two-step self-assembling process for the construction of two-component NPs that are well-dispersed under physiological pH.[24] The designed trigonal

Special Issue: Materials for Biological Applications

Received: September 22, 2011
Revised: December 2, 2011
Published: December 6, 2011

   dx.doi.org/10.1021/cm202860h | *Chem. Mater.* 2012, 24, 946−953

molecule can be prepared by coupling 9-fluorenylmethoxycarbonyl (Fmoc) groups with three legs of tris(2-aminoethyl)-amine (TAEA) with a one-step reaction. The resulting simple trigonal Fmoc-conjugate, FTAEA (Figure 1), can self-assemble

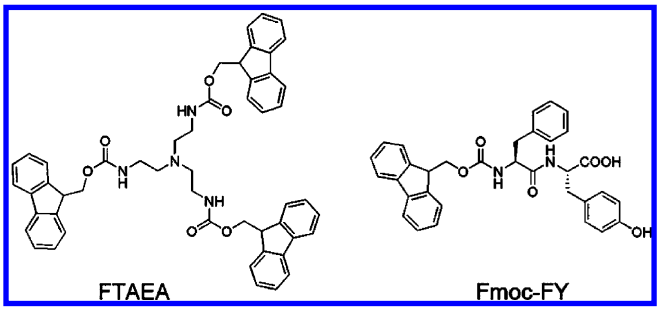

Figure 1. Chemical structures of self-assembling building blocks: FTAEA and Fmoc-FY.

efficiently into NPs in water with a low polydispersity index within seconds. An Fmoc-dipeptide, Fmoc-phenylalanine-tyrosine (Fmoc−FY), can further assemble around FTAEA NPs and stabilize them to form two-component NPs at physiological pH. In this work, we first demonstrated the excellent stability of the two-component NPs upon heating, incubation at 37 °C, long-time storage, and extreme dilution, which is vital to biomedical applications.

This advantage in stability further motivated our effort to generalize the stabilizer to biofunctional peptides, in order to fully exploit these new nanoparticles for drug delivery and biosensing. It was noticed that, without the stabilizer Fmoc-FY, FTAEA NPs would form precipitates at physiological pH. Fmoc-FY carries aromatic groups and is a self-assembling peptide.[25] However, it is not clear whether other oligopeptides can be used as stabilizers, and, if so, what characteristics they should possess. If these questions can be addressed, we have a facile and versatile method to prepare biofunctionalized NPs because of the simplicity of the system.

With the goal to explore essential features related to biomedical applications for the new nanoparticles, we have three objectives in this study: 1) demonstrating the stability of the two-component NP system; 2) exploring the general design criteria of oligopeptides critical for NP stabilization; 3) showing that the oligopeptide stabilizers possess a dual role of stabilization and functionalization, that is, they would display the expected bioactivity in live cell culture after the assembly on the NPs.

After systematically testing a series of molecules as stabilizers, we proposed the fundamental criteria for the design of stabilizing building blocks. Based on which, two functional sequences, Fmoc-phenylalanine-cysteine (Fmoc-FC) and Fmoc-phenylalanine-arginine-glycine-aspartic acid (Fmoc-FRGD), were designed and tested. The cysteine on the sequence is expected to confer mucoadhesive property[26] and also provides a binding site with inorganic colloids.[27,28] The sequence of RGD is originally identified as a cell-binding site in the extracellular matrix[29,30] and is known for binding with $\alpha_v\beta_3$ integrin receptor with high affinity. Because of the overexpression of integrin in a number of tumor cell types, RGD is useful for improving the diagnostic and therapeutic efficacy against cancer.[16,31,32] Fmoc-FRGD stabilized NPs were further evaluated for their bioactivity of cellular targeting in live cell culture.

EXPERIMENTAL SECTION

Materials. All Fmoc protected amino acids and peptides except Fmoc-FY and Fmoc-FYp were supplied by GL Biochem (Shanghai, China). All cell culture reagents were bought from Invitrogen. N,N′-Dicyclohexylcarbodiimide (DCC), N-hydroxysuccinimide (NHS), and other chemicals were purchased from Sigma-Aldrich unless otherwise stated. Water was prepared from Thermo Scientific Barnstead Nanopure ultrapure water purification system. The synthesis of FTAEA, Fmoc-FY, and Fmoc-FYp followed previous reports.[24,25]

Preparation of Two-Component NPs. FTAEA and Fmoc-FY were first dissolved in DMF to give stock solutions of the concentrations at 40 mM and 80 mM respectively. To fabricate FTAEA NPs, FTAEA stock solution (0.25 μL) was added into 100 μL of water with vortexing. To produce two-component NPs stabilized by Fmoc-FY, Fmoc-FY stock solution (0.125 μL) was added into 100 μL of phosphate buffer (PB, 20 mM, pH 7.4) with vortexing, and then the solution was added into 100 μL of the solution of FTAEA NPs drop by drop with vortexing. The preparation of two-component NPs stabilized by other molecules followed the same procedure.

Preparation of NR-RGD-NPs and NR-RDG-NPs. A stock solution containing 20 mM FTAEA and 200 μM Nile red (NR) in DMF was first prepared. Then the stock solution (0.6 μL) was added into 100 μL of water with vortexing. Fmoc-FRGD stock solution (0.15 μL) was added into 100 μL of PB solution with vortexing, and the solution was added into 100 μL of the above solution drop by drop with vortexing, which formed NR-RGD-NPs. To prepare NR-RDG-NPs, Fmoc-FRDG was used instead of Fmoc-FRGD. The concentration of FTAEA, Fmoc-FRGD, and Fmoc-FRDG of these samples is 60 μM, and NR concentration is 600 nM.

Testing Free Fmoc-FRGD and NR in the Solution of NR-RGD-NPs. One milliliter of the above NR-RGD-NP solution was dialyzed using a dialysis membrane tubing (Spectra Por, MWCO: 12000−14000, flat width: 25 mm) against 100 mL of PB (10 mM, pH 7.4). After 4 h of dialysis, the solution outside the tubing was taken for high-performance liquid chromatography (HPLC) and fluorescence spectroscopy analysis. The concentration of Fmoc-FRGD was determined by reverse-phase HPLC (Vydac C-18, 250 × 10 mm column) eluting with CH_3CN/water containing 0.1% TFA (starting from 35/65 to 45/55 over 20 min and then 100% CH_3CN from the time point of 21 min with a flow rate of 0.2 mL/min). The concentration of NR was determined by a spectrofluorometer (Perkin-Elmer LS 50B) with a Xenon discharge lamp excitation. The tested solution (400 μL) was mixed with 400 μL of DMF. The mixed solution was exited at 570 nm, and the emission was recorded at 650 nm. The experiments were repeated three times independently.

Dynamic Light Scattering (DLS). Both number average diameter and zeta potential measurements were performed on Zeta Plus (Brookhaven Instruments Corp. (BIC)). For diameter measurement, the BIC Particle Sizing Software was used. The prepared solution (100 μL) was put into a cuvette (Eppendorf UVette) and tested at 25 °C with a detection angle of 90 degrees and a wavelength of 659 nm. Each sample was run for 10 times with 15 s per run. The data of each run were collected only when its baseline index was larger than or equal to 5. All experiments were repeated at least three times independently.

To monitor the stability of NPs with temperature, Measurement Automation Setup was chosen with the starting temperature and temperature increment being 25 and 3 °C, respectively.

For the zeta potential test, the program of BIC PALS Zeta Potential Analyzer was used. The prepared solution (1.7 mL) was put into a big cuvette and tested at 25 °C. Each sample was run for 10 times with 10 cycles per run. All experiments were repeated at least three times independently.

Transmission Electron Microscopy (TEM). A 5 μL aliquot of the solution of NPs was deposited on a carbon-coated copper grid. After 2 min, excess solution was removed by a filter paper. The remainder was dried in a desiccator. The sample was then viewed using a JEOL 100CXII electron microscope operating at 80 kV or a JEOL 2010 electron microscope operating at 120 kV.

dx.doi.org/10.1021/cm202860h | Chem. Mater. 2012, 24, 946−953

Cryo-TEM Imaging. The measurements were conducted on an FEI/Philips Tecnai 12 BioTWIN transmission electron microscope, operating at 120 kV. Samples were prepared by a blotting procedure at room temperature and around 90% relative humidity. In a typical measurement, the sample solution (10 μL) was deposited on a copper grid coated by a lacey carbon film. Excess solution was blotted by a filter paper. The sample was immediately plunged into liquid propane cooled by liquid nitrogen, and the vitrified sample was transferred to the microscope with the protection of liquid nitrogen. Images were taken under low-dose conditions to minimize radiation damages to the samples.

Confocal Fluorescence Microscopy. To image the solution of NR-RGD-NPs, a 10 μL aliquot of the solution was deposited on a glass slide and covered by a coverslip. The sample was then imaged using a Zeiss laser scanning confocal microscope (LSM7 DUO (710+LIVE)) with an excitation wavelength of 561 nm. Other particle solutions were imaged using the same method.

For cell imaging, MDA-MB-435 cells were cultured in Dulbecco's modified Eagle medium (DMEM) supplemented with 10% fetal bovine serum (FBS) in a humidified atmosphere with 5% CO_2 at 37 °C. Cells were seeded on a 6-well plate with a coverslip on the bottom at a density of 30,000 cells per well. After an overnight incubation, the growth medium was replaced with the mixture of 900 μL of the above FBS-contained medium and 100 μL of the solution of NR-RGD-NPs or NR-RDG-NPs. After 2 h of incubation at 37 °C, cells were washed two times with the medium. Then the coverslip was put on a glass slide with the cell side face downward. The cells were then imaged by the confocal microscope with an excitation wavelength of 561 nm. The experiment of comparing cellular uptake for different samples was repeated three times independently.

The fluorescence images were quantitatively analyzed by the Image J program (National Institutes of Health, Bethesda) to compare the difference of fluorescence intensity. Confocal microscopic images were first exported as TIF files from the imaging software Zen 2009 (Carl Zeiss Microscopy). With Image J, these RGB images were then converted to an 8-bit binary format. The background color in different images was set with a threshold in the Adjust tool. Two items, Integrated Density and Limit to Threshold, in Set Measurement dialogue were selected, and the integrated density was measured from the remaining pixels that have the gray value larger than the threshold value. The fluorescence intensity of one image was considered to be proportional to the integrated density of the image. Therefore, the fluorescence intensity per cell in each image was calculated from the integrated density divided by the number of cells.

RESULTS AND DISCUSSION

The stability of two-component NPs stabilized by Fmoc-FY was traced by DLS analysis and TEM imaging. When the temperature increased from 25 to 70 °C at an average increasing rate of 1 °C min^{-1}, the diameter did not have significant change (Figure 2a). The unchanged size reveals the good thermostability of the two-component NPs. The two-component NPs also present a high stability upon dilution (Figure 2b). The solution of the two-component NPs shows a similar size when it was diluted with PB solution (10 mM, pH 7.4) by 10-fold and 100-fold to a final concentration of 5 μM and 500 nM. The diluted solutions at the concentration of 50 nM and 5 nM did not present reliable DLS data due to the weak signal collected from the diluted solutions. However, TEM imaging demonstrated that the diluted solution at the concentration of 5 nM still contained intact and well dispersed NPs (see Figure S1 in the Supporting Information). The good stability under conditions of extreme dilution is desired for drug delivery carriers following physiological administration where dilution happens in the circulatory system.[33]

When incubated at 37 °C for one week, the two-component NPs showed unaffected morphology as shown from the cryo-TEM image (Figure 2c). DLS results revealed that large particles started to form after one week of incubation at 37 °C (see Figure S2 in the Supporting Information). When two-component NPs were stored at 4 °C, their shelf life was extended to more than three months with no aggregation occurring, as verified by DLS analysis (see Figure S3 in the Supporting Information). Figure 2d shows the TEM image of the two-component NPs that were stored for twelve weeks at 4 °C. NPs were intact and no aggregate was observed. The good stability of the two-component NPs in aqueous phase facilitates their applications in biomedical fields. This exceptional stability of the NPs may be explained with the strong driving force for the NP formation, which is from the aromatic interactions among Fmoc groups in this system.[24] Aromatic interactions are expected to be strong in water because of the hydrophobic component of the interactions and electrostatic interactions between aromatic rings.[34]

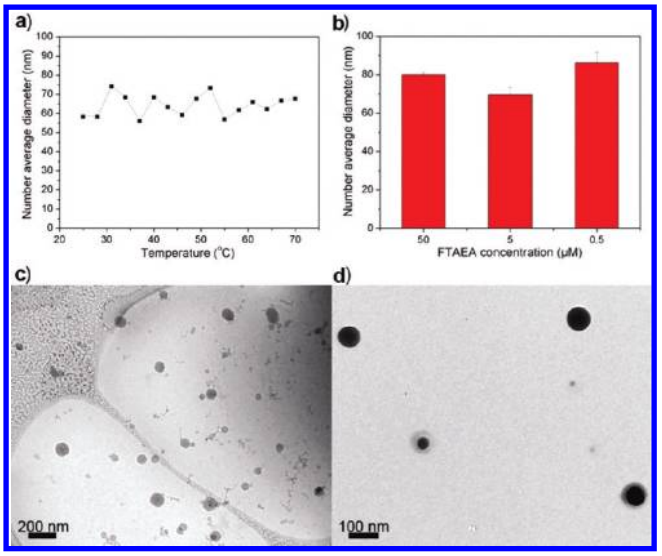

Figure 2. Stability analysis of the two-component NPs stabilized by Fmoc-FY. a), Number average diameters of two-component NPs with increasing temperature. b), Number average diameters of the two-component NPs with different FTAEA concentrations. The solutions with FTAEA concentration of 5 μM and 0.5 μM were prepared by diluting the solution where the concentration of FTAEA and Fmoc-FY is 50 μM. From two sample t test, there is no significant difference between any two samples ($P > 0.05$). Error bars indicate standard error of the mean ($n = 3$). c), Cryo-TEM image of the two-component NPs that were incubated at 37 °C for one week. d), TEM image of the two-component NPs that were stored at 4 °C for twelve weeks. The final concentration of FTAEA and Fmoc-FY of all samples is 50 μM.

In addition to stability, we aim to demonstrate the feasibility and versatility of adding bioactivity and functionality to the new nanocarriers. Our new approach in preparing nanoparticles makes use of two aromatic-complementary molecules: one responsible for the structural formation of the spherical core and the other as a corona stabilizer for dispersing the nanoparticles in aqueous phase at neutral pH. Furthermore, the molecules are used in a stepwise manner: the shape and size of the NPs are fixed in step 1, and the surface properties of NPs in step 2. This modular system should enable us to focus on the design of the stabilizers for modifying the functionalization of NPs, provided that we maintain the aromatic complementarity between the two modules.

To identify the design criteria of the stabilizers, we first began by examining Fmoc-FY, the stabilizer that we previously

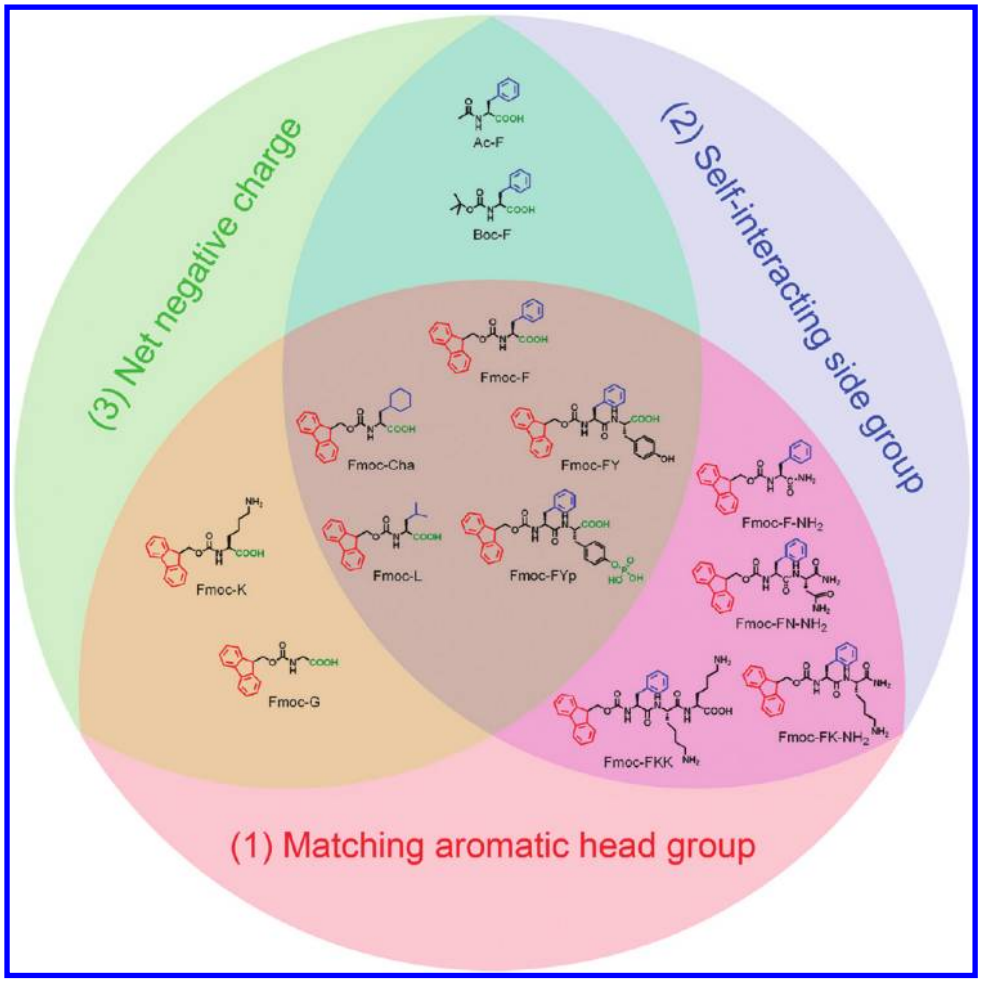

Figure 3. Chemical structures of tested molecules as stabilizers, which are grouped based on three characteristics. Molecules located in light red area contain a matching aromatic headgroup, Fmoc (presented in red). Molecules located in light blue area contain a self-interacting group, an aromatic or hydrophobic side chain (presented in blue). Molecules located in light green area contain a hydrophilic part with net negative charges, a carboxyl or phosphate group (presented in green). Molecules only containing the three characteristics (in the three-color-overlapped area) can be used as stabilizers.

reported.[24] The three characteristics that stand out are as follows: the presence of the aromatic headgroup, Fmoc, the presence of aromatic side chain in phenylalanine, and the presence of the negatively charged carboxyl terminal. One may reason the role of each one: Fmoc is for the matching aromatic interaction with FTAEA NPs, the core of the two-component NPs. The phenyl group may increase the stability of the assembly of the stabilizers themselves through self-interaction among aromatic groups,[35] and the carboxyl group serves to increase the hydrophilicity and achieves electrostatic stabilization.[24,36]

Fmoc-FY, however, is not the simplest molecule that possesses these three characteristics. Fmoc-phenylalanine (Fmoc-F) is the result of further trimming (Figure 3). Indeed, Fmoc-F was found capable of stabilizing FTAEA NPs and formed two-component NPs with a diameter of around 77.6 nm (Figure 4). The result suggests that molecules containing these three characteristics can be used as stabilizers. Next, we analyzed the necessity of each characteristic by designing and testing 11 more molecules (Figure 3). First, we replaced the Fmoc group with either N-acetyl (Ac) or N-(tert-Butoxycarbonyl) (Boc) group.[24] The resulting molecules, Ac-F and Boc-F, could not stabilize FTAEA NPs, and big aggregates were detected from DLS testing when the two molecules were used (Figure 4).

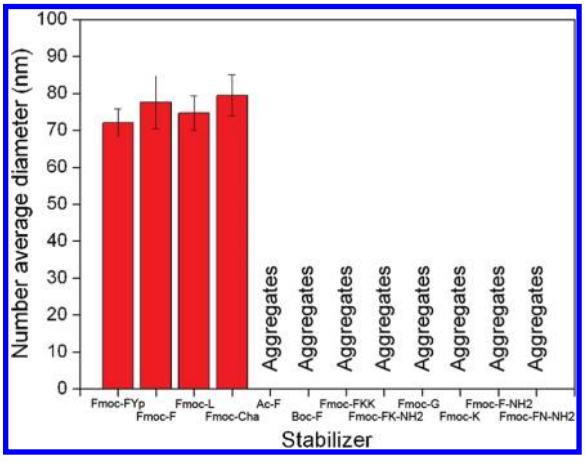

Figure 4. DLS results of two-component NPs stabilized by tested molecules. The column presents the number average diameter of NPs. Error bars indicate standard error of the mean (n = 3). The word, aggregates, means that the size of more than 1.0 μm was detected by DLS when the corresponding stabilizer used.

This indicates the necessity of Fmoc headgroup as a matching aromatic moiety to interact with FTAEA NPs.

dx.doi.org/10.1021/cm202860h | *Chem. Mater.* 2012, 24, 946–953

Next, we probe the effect of aromatic interaction among side chains. Fmoc-cyclohexylalanine (Fmoc-Cha) was tested because it is similar to Fmoc-F in size and shape but is nonaromatic and more hydrophobic.[37] Interestingly, Fmoc-Cha was found a suitable stabilizer, and two-component NPs of around 79.5 nm in diameters were formed with Fmoc-Cha as the stabilizer (Figure 4). The result suggests that the hydrophobic interaction in addition to the aromatic interaction can contribute to sufficient self-interaction effect among these molecules. To further validate this statement, we test another Fmoc-amino acid with a hydrophobic group on the side chain, Fmoc-leucine (Fmoc-L). Again, Fmoc-L could stabilize FTAEA NPs and formed two-component NPs with a number average diameter of around 74.7 nm (Figure 4), confirming that the requirement of self-association can be relaxed to include hydrophobic side chains. Other molecules whose side chains cannot form hydrophobic or aromatic interactions were analyzed to probe whether the self-interaction among side groups is a critical requirement. Fmoc-glycine (Fmoc-G) and Fmoc-lysine (Fmoc-K, isoelectric point is around 6.4), carrying neither aromatic nor hydrophobic group on the side chain, were found unsuitable as stabilizers for FTAEA NPs (Figure 4). Thus, a self-interacting side group is necessary for the design of stabilizers.

As stabilizers help to disperse NPs in aqueous phase, they should be hydrophilic and have good aqueous solubility. We reason that for both Fmoc-F and Fmoc-FY, the carboxyl terminal increases the hydrophilicity. The net charge on the NPs conferred by the negatively charged stabilizers provides electrostatic force against NP aggregation.[24] To check whether this statement holds, we replaced the carboxyl group with neutral group to obtain molecules without any charge: Fmoc-phenylalanine with amidated C-terminal (Fmoc-F-NH_2) and Fmoc-phenylalanine-asparagine with amidated end (Fmoc-FN-NH_2). As expected, these molecules exhibited poor water solubility and could not stabilize FTAEA NPs at neutral pH (Figure 4). Next, we differentiated between different charges. Fmoc-phenylalanine-lysine-lysine (Fmoc-FKK) and Fmoc-phenylalanine-lysine with C-terminal amidated (Fmoc-FK-NH_2) were designed to represent molecules with a net positive charge at pH 7.4. They were found unable to stabilize FTAEA NPs (Figure 4). Since FTAEA NPs carry a net positive charge, there is unfavorable enthalpic interaction between the core and the positively charged Fmoc-peptides. Compared to Fmoc-FY, Fmoc-phenylalanine-tyrosine-phosphate (Fmoc-FYp) is a molecule with an additional negatively charged group and is more hydrophilic at pH 7.4. Fmoc-FYp has been reported previously as capable of self-assembling but at a lower extent when compared with Fmoc-FY due to the presence of a hydrophilic phosphate group.[25,38] DLS result demonstrates that Fmoc-FYp can also stabilize FTAEA NPs and form two-component NPs with diameters of around 72.0 nm (Figure 4). The result indicates that the addition of phosphate group with more negative charges does not interrupt the stabilization effect. Negative charges of these stabilizers provide the electrostatic interaction with the positive charges of FTAEA NPs at pH 7.4 and meanwhile provide the electrostatic stabilization for the NPs.

According to the analysis and summary (Figure 3), we propose three fundamental criteria for the design of the stabilizing building block: (1) the molecule should contain a matching aromatic group (Fmoc in this case) to interact favorably with the spherical core; (2) the molecule should carry self-interacting (aromatic or hydrophobic) side group to maintain the stability of its own assembly on the particle surface; (3) the molecule should carry a net negative charge for favorable electrostatic interaction with the core and improvement of the NP dispersion in aqueous phase at neutral pH.

From the proposed criteria, we reason that oligopeptide sequence with a net negative charge (considering both side chains and C-terminal) conjugated to Fmoc-F should stabilize FTAEA NPs and provide corresponding biofunctionalities. To validate the criteria, we first designed a thiol-containing sequence, Fmoc-FC (Figure 5a). We confirmed that Fmoc-

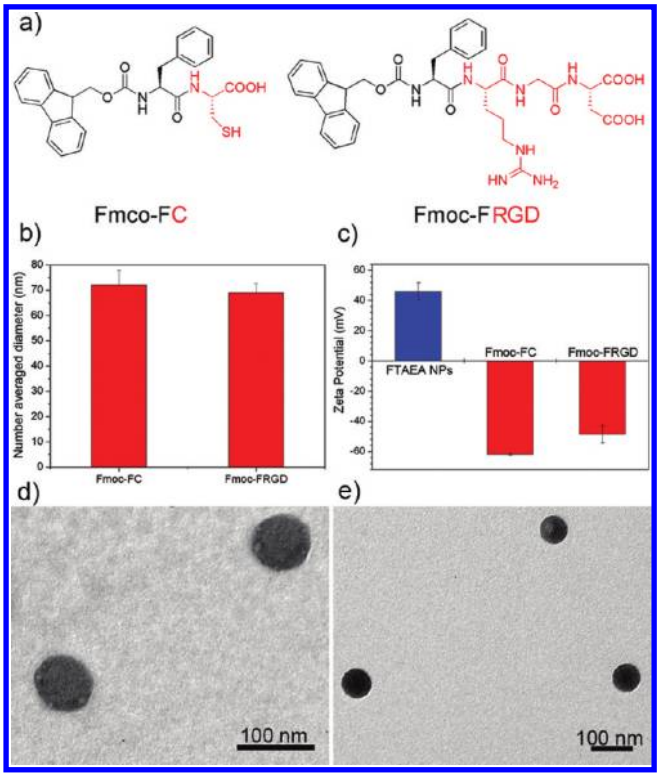

Figure 5. a), The chemical structures of the stabilizing building blocks with biofunctional groups indicated in red, Fmoc-FC and Fmoc-FRGD. b), Number average diameters of two-component NPs stabilized by Fmoc-FC and Fmoc-FRGD, respectively. c), Zeta potential of FTAEA NPs in water and two-component NPs in PB solution (pH 7.4) stabilized by Fmoc-FC and Fmoc-FRGD, respectively. Error bars indicate standard error of the mean (n = 3). TEM images of the two-component NPs stabilized by Fmoc-FC (d) or Fmoc-FRGD (e). The final concentration of FTAEA, Fmoc-FC, and Fmoc-FRGD of all samples is 50 μM.

FC could stabilize FTAEA NPs and produced two-component NPs with a number average diameter of 72.0 ± 5.8 nm (Figure 5b) and a zeta potential of −62.0 ± 0.5 mV (Figure 5c). Next, a cell-adhesion peptide sequence, RGD, was conjugated with Fmoc-F to yield a bioactive stabilizer, Fmoc-FRGD (Figure 5a). As expected, we found that FTAEA NPs could be stabilized by Fmoc-FRGD to form two-component NPs with a number average diameter of 69.0 ± 3.7 nm (Figure 5b) and a zeta potential of −48.9 ± 5.8 mV (Figure 5c). Compared with FTAEA NPs with a zeta potential of 46.0 ± 5.7 mV (Figure 5c), two-component NPs stabilized by Fmoc-FC or Fmoc-FRGD present a net negative charge, supporting that Fmoc-FC or Fmoc-FRGD are located on the surface of FTAEA NPs. Figure 5d and e presents the TEM images of well-dispersed two-component NPs stabilized by Fmoc-FC and

dx.doi.org/10.1021/cm202860h | Chem. Mater. 2012, 24, 946–953

Fmoc-FRGD, respectively. The results validate the stabilizer criteria and the possibility of incorporating bioactive peptide sequences into the stabilizer.

The successful functionalization of two-component NPs with Fmoc-FRGD is expected to endow the NPs with a promising targeting effect on tumor cells. This is true if the active sequence is properly oriented on the particle surface without hindrance. To examine the targeting function by fluorescence microscopy, we prepared NR-loaded Fmoc-FRGD functionalized FTAEA NPs (NR-RGD-NPs) in PB solution (see the movie in the Supporting Information). The DLS result shows a number average diameter of 73.6 nm with a polydispersity of 0.065 (Figure 6a). The TEM image of NR-RGD-NPs shows

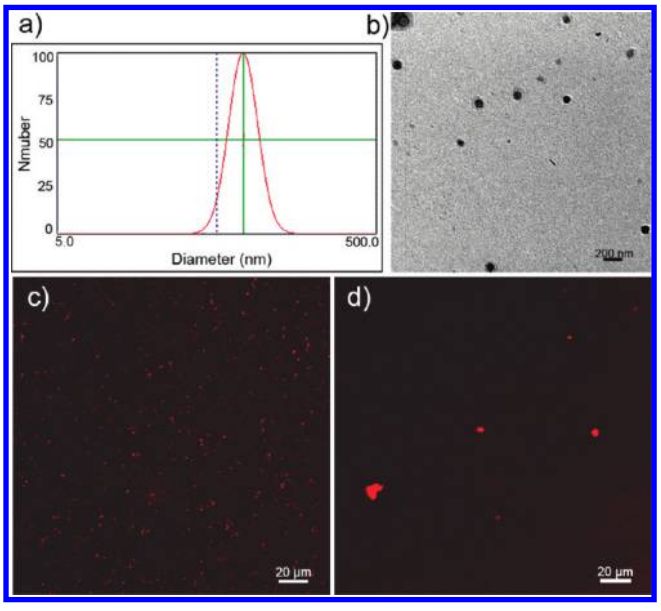

Figure 6. a), Distribution of hydrodynamic diameters of NR-RGD-NPs in PB solution. The result shows that the number average diameter is 73.6 nm with a polydispersity of 0.065. b), TEM image of NR-RGD-NPs in PB solution at pH 7.4. For sample (a) and (b), the concentration of FTAEA and Fmoc-FRGD is 60 μM, and NR concentration is 600 nM. Confocal fluorescence images of NR-RGD-NPs (c) and NR-NPs (d) in DMEM supplemented with 10% FBS. For sample (c) and (d), the concentration of FTAEA or Fmoc-FRGD is 6 μM, and NR concentration is 60 nM.

well-dispersed spherical NPs (Figure 6b). We used a dialysis method to separate the free molecules, Fmoc-FRGD and NR, from NR-RGD-NPs and tested their amount. With HPLC analysis, we determined that around 60.8% of Fmoc-FRGD did not bind to the NPs, where the ratio of bound Fmoc-FRGD to FTAEA is around 39.2/100. The result is reasonable as we have previously reported that FTAEA NPs still can be stabilized when the ratio of Fmoc-FY to FTAEA is 1/25.[24] Fluorometric analysis showed that around 8.4% NR were not incorporated into the NPs. This result reveals that a high NR encapsulation efficiency of around 91.6% is achieved by our NP system. We further tested whether the NPs could be dispersed in cell culture medium without aggregation. Figure 6c presents the confocal fluorescence image of NR-RGD-NPs in Dulbecco's modified Eagle medium (DMEM) supplemented with 10% fetal bovine serum (FBS). This image is similar to that of NR-RGD-NPs in PB solution (see Figure S4 in the Supporting Information). Since the fluorescence of NR depends on the hydrophobicity of the surrounding environment and is

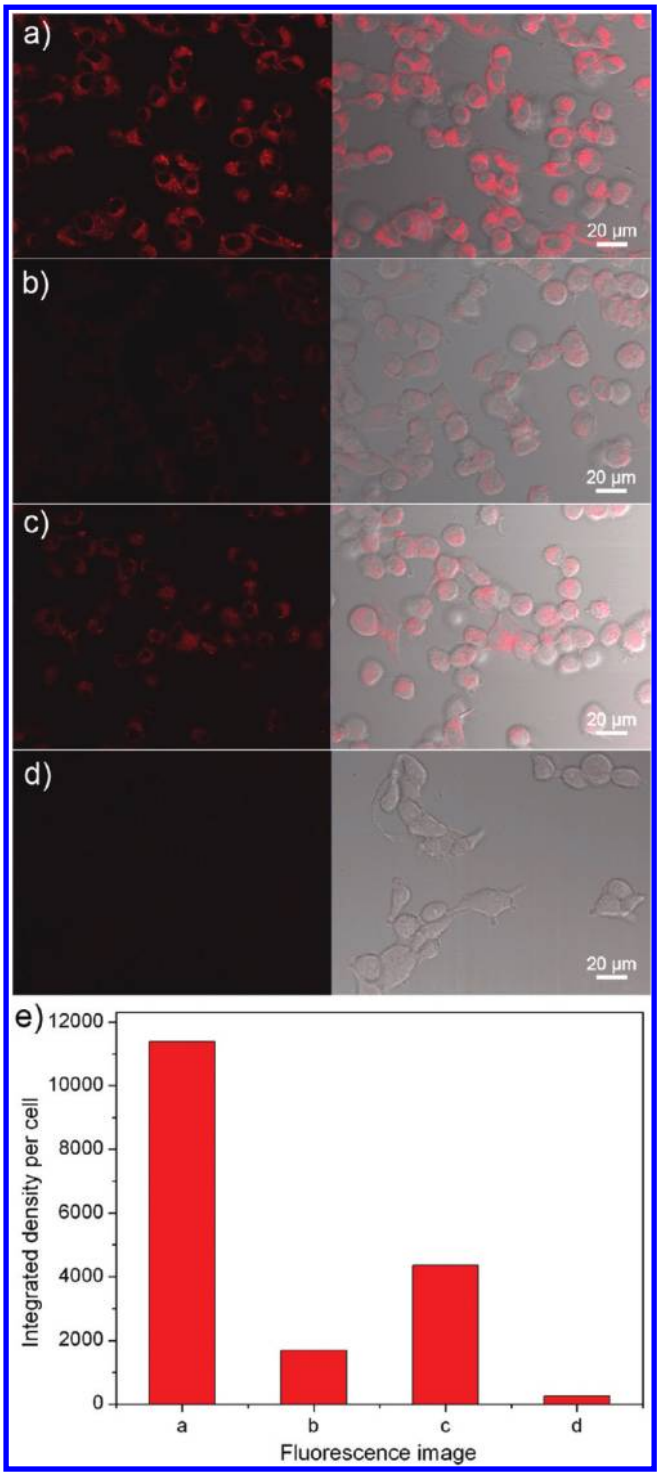

Figure 7. Confocal microscopy images of MDA-MB-435 cells after 2 h of incubation with NR-RGD-NPs at 37 °C (a), NR-RDG-NPs at 37 °C (b), NR-RGD-NPs with 20-fold of Fmoc-FRGD more than that in the sample of NR-RGD-NPs at 37 °C (c), and NR-RGD-NPs at 4 °C (d). The concentration of NR in all samples is 60 nM. Each panel shows a fluorescent image (left) and an overlaying image of brightfield and fluorescent images (right). e) Quantitative analysis of the above fluorescence images by the Image J program. The experiment was repeated three times independently.

negligible when it is dissolved in water,[24] the red dots in these figures support that the NR molecules are entrapped within the NPs. Note also that the red dots are well dispersed in these images. In contrast, aggregation is obvious for NR-loaded

dx.doi.org/10.1021/cm202860h | *Chem. Mater.* 2012, 24, 946–953

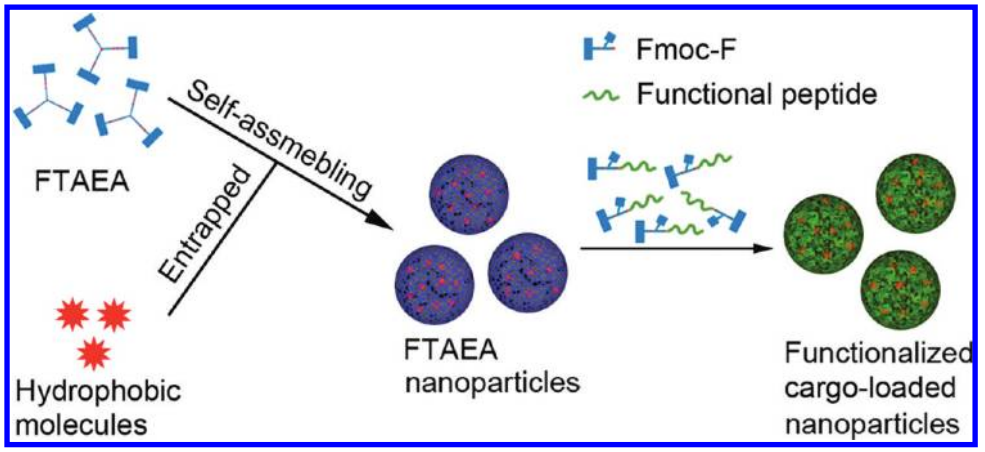

Figure 8. Schematic diagram of the construction of functionalized NPs with the entrapment of hydrophobic molecules.

NPs without Fmoc-FRGD stabilizers (NR-NPs) in the same medium (Figure 6d). The comparison further demonstrates the effect of Fmoc-FRGD for stabilizing the NPs. The stability of NR-RGD-NPs in the medium at 37 °C was evaluated by DLS. No aggregate was detected after 3 days of incubation (see Figure S5 in the Supporting Information), which reveals that the stability of our NPs outperforms that of general liposome systems.[39,40]

To evaluate the targeting effect of NR-RGD-NPs on cancer cells, the uptake of NR-RGD-NPs by human carcinoma cells (MDA-MB-435) was compared to the uptake of NR-loaded Fmoc-FRDG functionalized NPs (NR-RDG-NPs). MDA-MB-435 cell line is known for its overexpression of integrin receptor $\alpha_v\beta_3$.[41] The peptide RGD but not RDG shows high binding affinity to the integrin receptor $\alpha_v\beta_3$.[42,43] As a negative control, NR-RDG-NPs were prepared with the same method as NR-RGD-NPs. NR-RDG-NPs have a number average diameter of 72.6 nm with a polydispersity of 0.064, which is similar to that of NR-RGD-NPs (see Figure S6 in the Supporting Information). Figure 7a and b shows that NR-RGD-NPs were differentially taken up by the cells compared to NR-RDG-NPs, taking into account that NPs with the same concentration were added to the cells in each case. The result indicates that the bioactivity of RGD is preserved on the surface of NR-RGD-NPs. It implies that Fmoc-FRGD must be exposed on the particle surface and that the interaction with FTAEA core and the self-interaction among the stabilizer sequences do not hinder the proper presentation of RGD to the integrin receptors overexpressed on the cancer cells. Parallel competitive inhibition experiments were set up, in which excessive free Fmoc-FRGD was added together with NR-RGD-NPs. The fluorescence signal is weaker than that of NR-RGD-NPs sample (Figure 7a and c), supporting that the enhanced cellular uptake is mediated by integrin receptors that recognize RGD. Moreover, the fluorescent signal is negligible when the uptake experiment was performed at 4 °C (Figure 7d), indicating that the uptake of the NPs by MDA-MB-435 cells is an energy-dependent endocytic process. Figure 7e presents the quantitative analysis of the fluorescence images, which confirms the difference in cellular uptake between the different samples or conditions.

The facile process for preparing functionalized NPs with the entrapment of hydrophobic molecules is summarized in Figure 8 and also demonstrated in the movie (see the Supporting Information). Fmoc-conjugate, FTAEA, a trigonal molecule synthesized from a one-step reaction can efficiently self-assemble into NPs.[24] To entrap hydrophobic molecules with the NPs, they are simply added together with FTAEA first, and then they are entrapped during molecular assembling process in the first step. In the second step, which captures the key findings from this paper, negatively charged biofunctional oligopeptide conjugated with Fmoc-phenylalanine is added to stabilize cargo-loaded FTAEA NPs, resulting in functionalized NPs at physiological pH. The functionalization process only takes less than one minute, takes place in aqueous phase, and involves no chemical conjugation. The use of Fmoc as the aromatic group for driving the self-assembly is appealing since Fmoc is a standard protecting group in conventional solid phase peptide synthesis, meaning that no extra workup is required to prepare the Fmoc-oligopeptide stabilizer. The resulting NPs present better stability than other nanocarriers constructed by small molecules, like liposomes.[39,40] Importantly, the NPs can display the biofunction of the oligopeptides.

■ CONCLUSION

In summary, we demonstrated a simple strategy to prepare peptide-functionalized NPs with sub-100 nm size, low polydispersity index, good stability upon heating, incubation at 37 °C, long-time storage, and extreme dilution, and cellular targeting capability. More importantly, the strategy provides a platform with the two-step aromatic-directed self-assembling process for us to readily introduce various functional peptides on the surface of NPs. We proposed and validated the fundamental criteria for the design of Fmoc-oligopeptide-based stabilizers. From the enhanced uptake of Fmoc-FRGD functionalized NPs by cancer cells, we confirmed the surface presentation of the stabilizer and the bioactivity of the oligopeptide. Since a large number of oligopeptides can be accommodated by the design criteria, we believe that this approach is versatile and should provide an easy path to tailor NPs for many different applications. Moreover, this approach may be generalized to other aromatic self-assembly systems, such as those based on naphthalene, pyrene, and even aromatic drug molecules.

■ ASSOCIATED CONTENT

Ⓢ Supporting Information

Movie showing the preparation of NR-RGD-NPs, TEM image and DLS results of two-component NPs upon dilution, incubation and storage, confocal image of NR-RGD-NPs in PB solution, and DLS results of NR-RGD-NPs in the medium

and NR-RDG-NPs in PB solution. This material is available free of charge via the Internet at http://pubs.acs.org.

AUTHOR INFORMATION

Corresponding Author

*Phone: +852-23588935. Fax: +852-23580054. E-mail: ying.chau@ust.hk.

ACKNOWLEDGMENTS

This work was supported by the Hong Kong Research Grant Council (RPC10EG30). We thank Mr. Yu Yu from the Hong Kong University of Science and Technology for help in producing the movie.

REFERENCES

(1) Lewin, M.; Carlesso, N.; Tung, C. H.; Tang, X. W.; Cory, D.; Scadden, D. T.; Weissleder, R. *Nat. Biotechnol.* **2000**, *18*, 410.
(2) Weissleder, R. *Science* **2006**, *312*, 1168.
(3) West, J. L.; Halas, N. J. *Annu. Rev. Biomed. Eng.* **2003**, *5*, 285.
(4) Lal, S.; Clare, S. E.; Halas, N. J. *Acc. Chem. Res.* **2008**, *41*, 1842.
(5) Liu, L. H.; Xu, K. J.; Wang, H. Y.; Tan, P. K. J.; Fan, W. M.; Venkatraman, S. S.; Li, L. J.; Yang, Y. Y. *Nat. Nanotechnol.* **2009**, *4*, 457.
(6) Peer, D.; Karp, J. M.; Hong, S.; FaroKhzad, O. C.; Margalit, R.; Langer, R. *Nat. Nanotechnol.* **2007**, *2*, 751.
(7) Gu, F. X.; Karnik, R.; Wang, A. Z.; Alexis, F.; Levy-Nissenbaum, E.; Hong, S.; Langer, R. S.; Farokhzad, O. C. *Nano Today* **2007**, *2*, 14.
(8) Davis, M. E.; Chen, Z.; Shin, D. M. *Nat. Rev. Drug Discovery* **2008**, *7*, 771.
(9) Johnston, A. P. R.; Such, G. K.; Ng, S. L.; Caruso, F. *Curr. Opin. Colloid Interface Sci.* **2011**, *16*, 171.
(10) Wood, K. C.; Azarin, S. M.; Arap, W.; Pasqualini, R.; Langer, R.; Hammond, P. T. *Bioconjugate Chem.* **2008**, *19*, 403.
(11) Ryu, J. H.; Jiwpanich, S.; Chacko, R.; Bickerton, S.; Thayumanavan, S. *J. Am. Chem. Soc.* **2010**, *132*, 8246.
(12) Sutton, D.; Nasongkla, N.; Blanco, E.; Gao, J. M. *Pharm. Res.* **2007**, *24*, 1029.
(13) Chen, K.; Conti, P. S. *Adv. Drug Delivery Rev.* **2010**, *62*, 1005.
(14) Yang, Y. L.; Adelstein, S. J.; Kassis, A. I. *Drug Discovery Today* **2009**, *14*, 147.
(15) Deutscher, S. L. *Chem. Rev.* **2010**, *110*, 3196.
(16) Pangburn, T. O.; Petersen, M. A.; Waybrant, B.; Adil, M. M.; Kokkoli, E. *J. Biomech. Eng.-Trans. ASME* **2009**, 131.
(17) Franzen, S. *Expert Opin. Drug Delivery* **2011**, *8*, 281.
(18) Shi, M.; Lu, J.; Shoichet, M. S. *J. Mater. Chem.* **2009**, *19*, 5485.
(19) Kocbek, P.; Obermajer, N.; Cegnar, M.; Kos, J.; Kristl, J. *J. Controlled Release* **2007**, *120*, 18.
(20) Ghotbi, Z.; Haddadi, A.; Hamdy, S.; Hung, R. W.; Samuel, J.; Lavasanifar, A. *J. Drug Targeting* **2011**, *19*, 281.
(21) Nobs, L.; Buchegger, F.; Gurny, R.; Allemann, E. *J. Pharm. Sci.* **2004**, *93*, 1980.
(22) Connal, L. A.; Kinnane, C. R.; Zelikin, A. N.; Caruso, F. *Chem. Mater.* **2009**, *21*, 576.
(23) Leung, M. K. M.; Such, G. K.; Johnston, A. P. R.; Biswas, D. P.; Zhu, Z. Y.; Yan, Y.; Lutz, J. F.; Caruso, F. *Small* **2011**, *7*, 1075.
(24) Wang, W. P.; Chau, Y. *Chem. Commun.* **2011**, *47*, 10224.
(25) Wang, W. P.; Yang, Z. M.; Patanavanich, S.; Xu, B.; Chau, Y. *Soft Matter* **2008**, *4*, 1617.
(26) Bernkop-Schnurch, A. *Adv. Drug Delivery Rev.* **2005**, *57*, 1569.
(27) Cao, R.; Diaz-Garcia, A. M.; Cao, R. *Coord. Chem. Rev.* **2009**, *253*, 1262.
(28) Lim, S. I.; Zhong, C. J. *Acc. Chem. Res.* **2009**, *42*, 798.
(29) Pierschbacher, M. D.; Ruoslahti, E. *Nature* **1984**, *309*, 30.
(30) Hersel, U.; Dahmen, C.; Kessler, H. *Biomaterials* **2003**, *24*, 4385.
(31) Pasqualini, R.; Koivunen, E.; Ruoslahti, E. *Nat. Biotechnol.* **1997**, *15*, 542.
(32) Pu, K. Y.; Li, K.; Liu, B. *Chem. Mater.* **2010**, *22*, 6736.
(33) Woodle, M. C. *Adv. Drug Delivery Rev.* **1995**, *16*, 249.
(34) Waters, M. L. *Curr. Opin. Chem. Biol.* **2002**, *6*, 736.
(35) Tatko, C. D.; Waters, M. L. *J. Am. Chem. Soc.* **2002**, *124*, 9372.
(36) Cousins, B. G.; Das, A. K.; Sharma, R.; Li, Y. N.; McNamara, J. P.; Hillier, I. H.; Kinloch, I. A.; Ulijn, R. V. *Small* **2009**, *5*, 587.
(37) McMenimen, K. A.; Petersson, E. J.; Lester, H. A.; Dougherty, D. A. *ACS Chem. Biol.* **2006**, *1*, 227.
(38) Wang, W. P.; Chau, Y. *Soft Matter* **2009**, *5*, 4893.
(39) Langer, R. *Science* **1990**, *249*, 1527.
(40) Sharma, A.; Sharma, U. S. *Int. J. Pharm.* **1997**, *154*, 123.
(41) Arap, W.; Pasqualini, R.; Ruoslahti, E. *Science* **1998**, *279*, 377.
(42) Shokeen, M.; Pressly, E. D.; Hagooly, A.; Zheleznyak, A.; Ramos, N.; Fiamengo, A. L.; Welch, M. J.; Hawker, C. J.; Anderson, C. J. *ACS Nano* **2011**, *5*, 738.
(43) VandeVondele, S.; Voros, J.; Hubbell, J. A. *Biotechnol. Bioeng.* **2003**, *82*, 784.